

Photocurrent, Space-Charge Buildup, and Field Emission in Alkali Halide Crystals*

A. VON HIPPEL, E. P. GROSS, J. G. JELATIS, AND M. GELLER

Laboratory for Insulation Research, Massachusetts Institute of Technology, Cambridge, Massachusetts

(Received March 18, 1953)

Additively colored alkali halide crystals represent, in a first approximation, a transparent solid with frozen-in electrons which can be mobilized by light absorption. When moving towards the anode, these electrons leave a positive space charge behind, and an adjustable cathode fall results which can be steepened until electrons are released by field emission. The steady-state and transient solutions for the charging and discharging cycle are calculated, the effects of light intensity, wavelength, and field emission discussed, and KBr crystals investigated experimentally as function of time, voltage, light intensity, and color-center density. Field emission has been produced with voltages as low as 1 volt, and a field-emission photocell has been realized.

INTRODUCTION

WHILE studying the mechanisms of electric breakdown, we have become increasingly interested in the formation of space charges, the release of electrons from the cathode, and their transconductance through the dielectric.¹ Space-charge phenomena, furthermore, are the key problem for the understanding of interfacial polarization and electret formation, and for the operation of dry rectifiers and transistors. If the field distortion could be observed in a transparent system and controlled at will, much useful insight would be gained.

Alkali halide crystals, permanently colored by F centers, can fulfill the prerequisites for such a system. Under the proper conditions they represent a transparent solid with frozen-in electrons which can be mobilized by light absorption. When moving towards the anode, these electrons leave behind halogen defects as positive countercharges. An adjustable voltage gradient results that can be steepened at the cathode until electrons are released from the metal electrode into the crystal. Space charges of any desired distribution may be created by selective, localized illumination, thus permitting the formation of rectifying boundaries and the reproduction of a variety of electret effects which, in opaque solids, puzzle the observer.

The present paper reports the first stages of this research project.

1. SPACE-CHARGE BUILD-UP BY PHOTOEFFECT UNDER IDEALIZED CONDITIONS

An alkali halide crystal, permanently and not too deeply colored in alkali vapor or by the release of electrons from the cathode at high temperature, fulfills, in a first approximation, the following conditions:

(1) The principal electron traps are uniformly dispersed anion vacancies; (2) only a small fraction of these traps is occupied; (3) the essential release mechanism is light absorption in the F band; thermal liberation of electrons from their traps may be neglected;

(4) the charge-carrier density depends only on the distance x between cathode ($x=0$) and anode ($x=l$) as long as the light absorption of the crystal, illuminated perpendicularly to the field, is small; (5) electrons may leave at the anode but not re-enter from the cathode; (6) conduction by ions and holes may be neglected.

In this situation our crystal represents a box containing, at the start, an electron cloud of uniform density, frozen into a compensating positive matrix. When a dc field is applied in the x direction, the voltage gradient is constant throughout, until, at $t=0$, a uniform illumination is switched on. Electrons now become mobilized, equal in number to the quanta absorbed times the quantum yield, and drift toward the anode until they are discharged or retrapped by anion vacancies. This motion of the electron cloud towards the anode leaves a bleached region of positive space charge behind. If the initial concentration of color centers is sufficiently small and the applied voltage sufficiently high, the final state will be a completely bleached crystal. For higher concentrations or lower voltages, the crystal in the end stage will consist of two distinct sections; a completely bleached positive region I in front of the cathode absorbing the total voltage drop, and a field-free, unbleached, neutral region II with the original color-center concentration (Fig. 1). Diffusion blurring the boundary between the regions I and II will be neglected for the present.

This final steady state of the field distribution can be calculated easily. If N_0 denotes the number of F centers per unit volume and e the elementary charge, we have in bleached region I a constant positive space-charge density

$$\rho_0 = N_0 e, \quad (1)$$

i.e., according to Poisson's equation, a constant field strength gradient²

$$(dE/dx)_1 = \rho_0 / \epsilon', \quad (2)$$

where ϵ' is the dielectric constant of the crystal. The field strength,

$$E_1 = (\rho_0 / \epsilon')(x - d_\infty), \quad (3)$$

* Sponsored by the U. S. Office of Naval Research, the U. S. Army Signal Corps, and the U. S. Air Force.

¹ A. von Hippel and R. S. Alger, *Phys. Rev.* **76**, 127 (1949).

² We use the rationalized mks system where the dielectric constant of vacuum is $\epsilon_0 = 8.854 \times 10^{-12}$ [farad m^{-1}].

decreases linearly with the distance x from the cathode and is concentrated in a cathode fall of the length d_∞ . Region II, unbleached, is free of space charge and of field,

$$(dE/dx)_2=0, \quad E_2=\text{const}=0. \quad (4)$$

The total voltage V_0 , applied initially across the geometrical length l of the crystal, has contracted across d_∞ in front of the cathode as

$$V_0 = - \int_0^l E dx = - \int_0^\infty \frac{\rho_0}{\epsilon'} (x - d_\infty) dx = \frac{\rho_0}{2\epsilon'} d_\infty^2. \quad (5)$$

Thus a cathode fall has formed of length

$$d_\infty = (2\epsilon' V_0 / \rho_0)^{1/2} \text{ [m]}, \quad (6)$$

in which the field strength reaches its maximum value,

$$E_c = -(\rho_0 / \epsilon') d_\infty \text{ [volt m}^{-1}\text{]}, \quad (7)$$

directly in front of the cathode.

An F -center concentration, $N_0 = 1 \times 10^{22} \text{ [m}^{-3}\text{]}$, may be a reasonable upper limit in view of conditions (2) and (4), and a static permittivity $\epsilon' = 6\epsilon_0$, a representative value for the alkali halides. By applying 1000 v across a crystal of 1-cm length, we contract, by illumination, the original field of uniform strength $E_0 = 1 \times 10^6 \text{ [volt m}^{-1}\text{]}$ into a cathode fall of length

$$d_\infty \simeq 8 \times 10^{-6} \text{ [m]},$$

and raise the field strength in front of the cathode to

$$E_c \simeq 2.5 \times 10^8 \text{ [volt m}^{-1}\text{]}.$$

This field strength exceeds the intrinsic breakdown strength of most alkali halide crystals;³ hence field emission is likely to set in and to arrest the further rise of the field before the breakdown strength is reached.¹ But obviously the simple expedient of creating a high-voltage gradient internally by controlled space-charge buildup instead of applying a comparable external field gives a new access to the "physics of high-field strength" without the difficulties usually encountered in high-voltage investigations.

2. TRANSIENT RESPONSE

The steady state produced by illumination leaves the crystal divided into two sections, a completely bleached cathodic region I and an unbleached anodic region II, abutting in a sharp boundary. We will assume that this division prevails also during the transient stage, i.e., that a "shock front" $x = d(t)$ separating regions I and II advances from the cathode and, slowing down, comes to rest at the distance $x = d_\infty$. This presupposes that we can lump summarily the photoelectric release of the electrons, their motion through the lattice and retrapping by halogen defects into an effective mobility b . Thus we have the model of an electron cloud of the

³ See A. von Hippel, J. Appl. Phys. 8, 815 (1937).

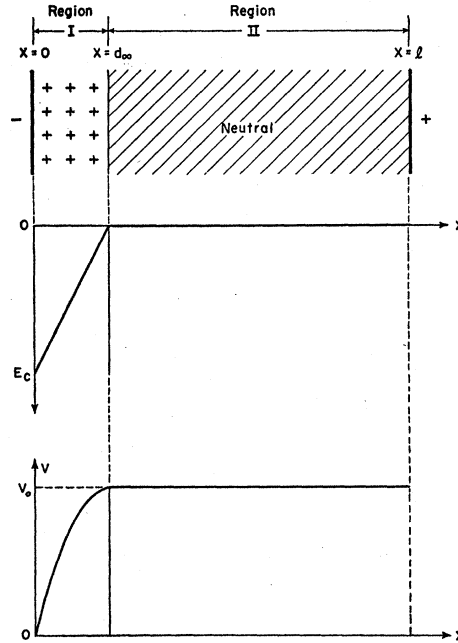


FIG. 1. Space charge, field strength, and voltage distribution in colored alkali halide crystal after charging (theoretical).

density ρ and mobility b , moving through a stationary cloud of positive charges of the density ρ_0 .

The electron cloud, according to Stokes' law, carries a current density

$$J = \rho b E; \quad (8)$$

the field-strength gradient, according to Poisson's equation, is

$$\partial E / \partial x = (\rho + \rho_0) / \epsilon' \quad (9)$$

with ρ negative; the condition of current continuity demands furthermore that

$$\partial \rho / \partial t = - \partial J / \partial x. \quad (10)$$

Substituting J from Eq. (8) we obtain the continuity condition in the form of the nonlinear differential equation

$$\partial \rho / \partial t + b \partial (\rho E) / \partial x = 0, \quad (11)$$

with the boundary conditions

$$\begin{aligned} \text{for } t=0: \quad \rho &= -\rho_0, \quad E = \text{const} = -V_0/l, \\ \text{for } t>0: \quad \rho(\text{at } x=0) &= 0, \quad \int_0^l E dx = -V_0. \end{aligned} \quad (12)$$

Region I, extending from $x=0$ to $x=d(t)$, has been vacated by the electron cloud [$\rho(x)=0$ for $x < d(t)$]; according to Eq. (9) the field strength is here

$$E_1 = (\rho_0 / \epsilon') x + C(t). \quad (13)$$

In the unbleached region II the space-charge densities of electron cloud and positive background cancel

$[\rho(x) = -\rho_0]$; hence the field strength in this section,

$$E_2 = D(t), \quad (14)$$

is independent of x and is a function of time only. At the shock front itself $[x = d(t)]$,

$$E_1 = E_2. \quad (15)$$

Hence

$$(\rho_0/\epsilon')d(t) + C(t) = D(t). \quad (16)$$

The boundary condition for $t > 0$ (Eq. 12) leads to a second equation between the position of the shock front $d(t)$ and the time-dependent voltage gradients in regions I and II:

$$\int_0^{d(t)} \left[\frac{\rho_0}{\epsilon'} x + C(t) \right] dx + D(t)[l - d(t)] = -V_0. \quad (17)$$

A third equation is obtained from the continuity condition, Eq. (11). Region I, stripped of moving charge carriers, is traversed only by a displacement current of density

$$\epsilon' \partial E_1 / \partial t = \epsilon' \partial C(t) / \partial t. \quad (18)$$

Region II carries a conduction and a displacement current:

$$-\rho_0 b E_2 + \epsilon' \partial E_2 / \partial t = -\rho_0 b D(t) + \epsilon' \partial D(t) / \partial t. \quad (19)$$

Current continuity requires that the total current passing through region I equals that through region II, or

$$\epsilon' \partial C(t) / \partial t = -\rho_0 b D(t) + \epsilon' \partial D(t) / \partial t \equiv J'. \quad (20)$$

Substituting $D(t)$ from Eq. (16) into Eqs. (17) and (20), we arrive at the two equations for $d(t)$ and $C(t)$:

$$\frac{\rho_0}{\epsilon'} d(t) + l C(t) - \frac{\rho_0}{2\epsilon'} [d(t)]^2 = -V_0, \quad (21)$$

$$-\frac{\rho_0 b}{\epsilon'} d(t) + \frac{\partial d(t)}{\partial t} = b C(t).$$

By eliminating $C(t)$ we finally obtain the differential equation for the motion of the shock front:

$$\frac{\partial d(t)}{\partial t} - \frac{\rho_0 b}{2l\epsilon'} [d(t)]^2 = -\frac{b}{l} V_0. \quad (22)$$

Its solution is

$$d(t) = \left(\frac{2\epsilon'}{\rho_0} V_0 \right)^{\frac{1}{2}} \frac{1 - \exp[-(2\rho_0 b^2 V_0 / \epsilon' l^2)^{\frac{1}{2}} t]}{1 + \exp[-(2\rho_0 b^2 V_0 / \epsilon' l^2)^{\frac{1}{2}} t]}. \quad (23)$$

For $t=0$, $d(t)=0$ as prescribed, i.e., the crystal is colored uniformly. For $t \rightarrow \infty$,

$$d(t) = (2\epsilon' V_0 / \rho_0)^{\frac{1}{2}} \equiv d_\infty, \quad (24)$$

in accordance with Eq. (6). The motion of the shock front itself is regulated by a relaxation time

$$\tau \equiv (2\rho_0 b^2 V_0 / \epsilon' l^2)^{-\frac{1}{2}}, \quad (25)$$

which has a simple physical interpretation. By introducing d_∞ from Eq. (24), the relaxation time may be written

$$\tau = d_\infty / 2bE_0 \equiv d_\infty / 2v_0. \quad (26)$$

Hence τ represents the time required for an electron to move with the drift velocity v_0 in the undistorted field E_0 through half the distance of the final cathode fall d_∞ . By introducing d_∞ and τ , Eq. (23) for the shock-front position becomes

$$d(t) = d_\infty \frac{1 - e^{-t/\tau}}{1 + e^{-t/\tau}} = d_\infty \tanh\left(\frac{t}{2\tau}\right). \quad (27)$$

The motion of the shock front may be determined visually by observing $d(t)$, if the cathode fall is of macroscopic length. Alternatively, it can be measured by the current $I(t)$ or the charge $Q(t)$ that traverses the external circuit. For a crystal of cross section A , the current is, according to Eqs. (20) and (21):

$$I(t) \equiv A J'(t) = \frac{A \epsilon'}{b} \left\{ \frac{\partial^2 d(t)}{\partial t^2} - \frac{\rho_0 b}{\epsilon'} \frac{\partial d(t)}{\partial t} \right\}, \quad (28)$$

or, by introducing $d(t)$ from Eq. (27), it is

$$I(t) = \frac{-2A\rho_0 d_\infty}{\tau} e^{-t/\tau} \left\{ \frac{(1 - e^{-t/\tau}) d_\infty / l + (1 + e^{-t/\tau})}{(1 + e^{-t/\tau})^3} \right\}. \quad (29)$$

At $t=0$, when the illumination has just been switched on, the current is at its maximum,

$$I(0) = -A\rho_0 d_\infty / 2\tau = -A\rho_0 v_0, \quad (30)$$

and equal to the conduction current traversing the crystal in the undistorted field.

Since, for our experiments, $d_\infty / l \ll 1$, Eq. (29) simplifies to

$$I(t) \simeq I(0) / \cosh^2(t/2\tau). \quad (29a)$$

Plotted as $\log I(t)$ vs $\zeta \equiv t/2\tau$, the characteristic deviates from a straight line only for $\zeta < 1$, where the slope curves towards zero (Fig. 2).

The charge transferred during the time t is [see Eq. (20)]:

$$Q(t) = \int_0^t I(t) dt = A \epsilon' \{ C(t) - C(0) \}. \quad (31)$$

Since, according to Eq. (21),

$$C(t) - C(0) = -\frac{\rho_0}{\epsilon'} d(t) + \frac{\rho_0}{2\epsilon' l} [d(t)]^2, \quad (32)$$

Eq. (31) may be rewritten

$$Q(t) = A\rho_0 d(t) \{ -1 + (1/2l)d(t) \}; \quad (33)$$

and the total charge transported through the crystal for $t \rightarrow \infty$ becomes

$$Q(\infty) = -(A\rho_0 d_\infty/l) \{l - \frac{1}{2}d_\infty\}. \quad (34)$$

This result has again a simple meaning. If the whole crystal had been bleached ($d_\infty = l$), $Q(\infty) = A\rho_0 l/2$, i.e., the total charge of the electron cloud would have been moved in effect across half the crystal length. Vice versa, for a very short cathode fall ($d_\infty \ll l$), $Q(\infty) \simeq A\rho_0 d_\infty$, i.e., the electron cloud has moved the distance of the cathode fall.

The field distribution in region I [$x \leq d(t)$], according to Eqs. (13) and (21), is

$$E_1 = -\frac{V_0}{l} + \frac{\rho_0}{\epsilon'} \left\{ (x - d(t)) + \frac{1}{2l} [d(t)]^2 \right\}. \quad (35)$$

For $t = \infty$, since

$$\rho_0 d_\infty^2 / \epsilon' 2l = V_0/l, \quad (36)$$

the field in the cathode fall becomes

$$E_1(\infty) = (\rho_0/\epsilon')(x - d_\infty), \quad (37)$$

as Eq. (3) of the steady-state solution prescribes. The field strength in region II, according to Eqs. (14) and (16), is

$$E_2 = -(V_0/l) \{1 - (d(t))^2/d_\infty^2\}; \quad (38)$$

it is independent of x and falls to zero at $t = \infty$. For $t = 0$, both fields are identical and equal to the undistorted field $E = -V_0/l$.

3. DISCHARGING AND RECHARGING

The preceding calculation describes the *initial* charging of a crystal. Any *subsequent* discharging and later recharging to the same voltage proceeds under altered conditions since only the first application of the field discharges electrons at the anode. From here on, as long as electrons may not re-enter from the cathode and the ions are frozen in, the space charge in the crystal adjusts itself to shorting and reapplication of the voltage V by a backward or forward motion of the electron cloud without charge transfer to the electrodes.

Let us illustrate the situation graphically. The charging process terminates in the steady-state condition shown in Fig. 1:

$$\text{for } x \leq d_\infty \quad \begin{cases} E_1(x) = (\rho_0/\epsilon')(x - d_\infty), \\ V_1(x) = -\int_0^x E_1 dx = (\rho_0/\epsilon')(d_\infty x - \frac{1}{2}x^2), \end{cases} \quad (39)$$

$$\text{for } d_\infty \leq x \leq l \quad \begin{cases} E_2(x) = 0, \\ V_2(x) = \rho_0 d_\infty^2 / \epsilon'^2 = V_0. \end{cases}$$

When, at the start of a discharging experiment, the external voltage is removed at $t = 0$ by short-circuiting the electrodes, we have to subtract from $E(x)$ the

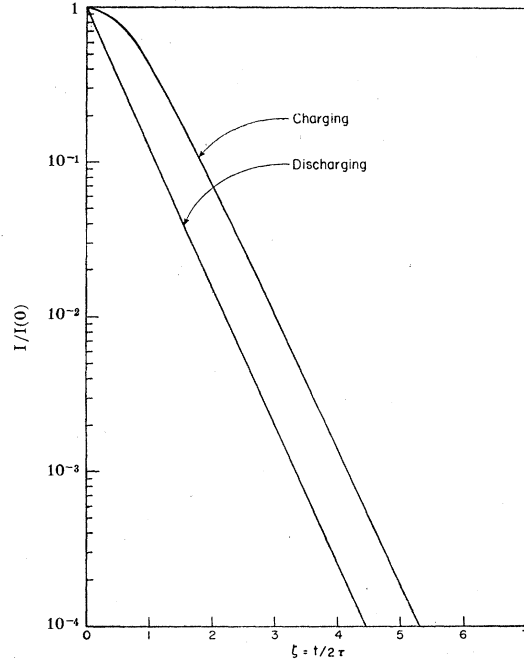


FIG. 2. Time dependence of photocurrent through colored alkali halide crystal (theoretical).

external field $-V_0/l$ and from $V(x)$ the external voltage $V_0 x/l$. Hence

$$\begin{aligned} \text{region I} & \begin{cases} E_1(x) = (\rho_0/\epsilon')(x - d_\infty) + V_0/l \\ V_1(x) = (\rho_0/\epsilon')(d_\infty x - \frac{1}{2}x^2) - V_0 x/l, \end{cases} \\ \text{region II} & \begin{cases} E_2(x) = V_0/l \\ V_2(x) = V_0(1 - x/l) \end{cases} \end{aligned} \quad (40)$$

(see Fig. 3). The voltage now reaches a maximum in the bleached region at the location

$$x_0 = d_\infty - V_0 \epsilon' / l \rho_0 = d_\infty (1 - d_\infty / 2l) \quad (41)$$

of the value

$$V_{1 \max} = (\rho_0 / 2 \epsilon') x_0^2, \quad (42)$$

and drops on both sides towards zero.

This situation is obviously not a stable one. When mobilized by illumination, the electron cloud will be pulled back by the space-charge field into a symmetrical position between the electrodes (Fig. 4). Region II again will become field free, and two unbleached regions I and III in front of the electrodes and of equal thickness $d_\infty/2$, will contain the voltage drop produced by the positive space charge. The steady state must be (for $t = \infty$)

$$\begin{aligned} E_1(x) &= (\rho_0/\epsilon')(x - \frac{1}{2}d_\infty), & V_1(x) &= (\rho_0/\epsilon')(\frac{1}{2}d_\infty x - \frac{1}{2}x^2), \\ E_2(x) &= 0, & V_2(x) &= \frac{1}{4}V_0, \\ E_3(x) &= -E_1(l-x), & V_3(x) &= +V_1(l-x). \end{aligned} \quad (43)$$

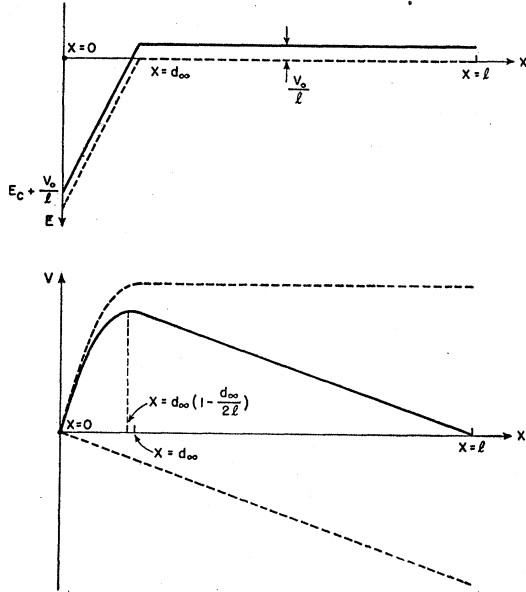


FIG. 3. Field and voltage distribution at beginning of discharge (theoretical).

The calculation of the transient response follows the pattern set in the preceding section. In analogy to Eqs. (13) to (15), we specify for the three fields:

$$\begin{aligned} E_1 &= (\rho/\epsilon')x + C(t) \quad [\text{for } x \leq d(t)], \\ E_2 &= D(t) \quad [\text{for } d(t) \leq x \leq l - d_\infty + d(t)], \\ E_3 &= (\rho/\epsilon')x + F(t) \quad [\text{for } l - d_\infty + d(t) \leq x \leq l], \end{aligned} \quad (44)$$

with the matching conditions

$$\begin{aligned} E_1(d(t)) &= E_2(d(t)), \\ E_2(l - d_\infty + d(t)) &= E_3(l - d_\infty + d(t)). \end{aligned} \quad (45)$$

Current continuity demands [see Eqs. (18) to (20)]

$$\epsilon' \partial C(t)/\partial t = \rho_0 b D(t) + \epsilon' \partial D(t)/\partial t = \epsilon' \partial F(t)/\partial t. \quad (46)$$

Furthermore, replacing Eq. (17), we require that the total voltage must be zero:

$$\begin{aligned} \{ (\rho_0/2\epsilon') [d(t)]^2 + C(t)d(t) \} + D(t)(l - d_\infty) \\ + \{ (\rho_0/2\epsilon') (l^2 - [l - d_\infty + d(t)]^2) \} \\ + F(t)[d_\infty - d(t)] = 0. \end{aligned} \quad (47)$$

Eliminating $C(t)$ and $D(t)$ we arrive at the differential equation for the shock front,

$$\partial d(t)/\partial t + d(t)d_\infty b \rho_0 / l \epsilon' = (b/l)V_0, \quad (48)$$

with the solution

$$d(t) = \frac{1}{2}d_\infty(1 + e^{-t/\tau}). \quad (49)$$

In contrast to the first charging, the displacement of the electron cloud follows now a simple exponential decay law (see Fig. 2) with the previous time constant [see Eq. (26)]:

$$\tau = d_\infty l / 2bV_0. \quad (50)$$

In consequence, the short-circuit current caused by the motion of the electron cloud [see Eq. (28)],

$$\begin{aligned} I(t) &= A \epsilon' \frac{dC(t)}{dt} = -\frac{A \epsilon'}{b} \left\{ \frac{\partial^2 d(t)}{\partial t^2} - \frac{\rho_0 b}{\epsilon'} \frac{\partial d(t)}{\partial t} \right\} \\ &= A \frac{\rho_0 d_\infty}{2t} \left(1 - \frac{d_\infty}{l} \right) e^{-t/\tau}, \end{aligned} \quad (51)$$

also shows a simple exponential decay. Its initial value, for $t=0$ and $d_\infty \ll l$, is identical with the maximum charging current of Eq. (30).

After the equilibrium situation of Fig. 4 is established, a reapplication of the voltage V_0 causes a transient described by the same equations as above, only the voltage $-V_0$ has to be introduced on the right side of Eq. (47). The shock front moves to the right again according to the exponential decay law

$$d(t) = d_\infty(1 - \frac{1}{2}e^{-t/\tau}), \quad (52)$$

with an identical current flow

$$I(t) = -A(\rho_0 d_\infty / 2\tau)(1 - d_\infty/l)e^{-t/\tau} \quad (53)$$

in the opposite direction. Hence, by applying an alternating field of the amplitude $V_0/2$, we should observe, as function of frequency, a simple relaxation spectrum caused by the space-charge motion in the crystal capacitor.

4. DEPENDENCE ON LIGHT INTENSITY AND WAVELENGTH

Since we specified that the electron cloud may be mobilized by light only (condition 3, Sec. 1), we have

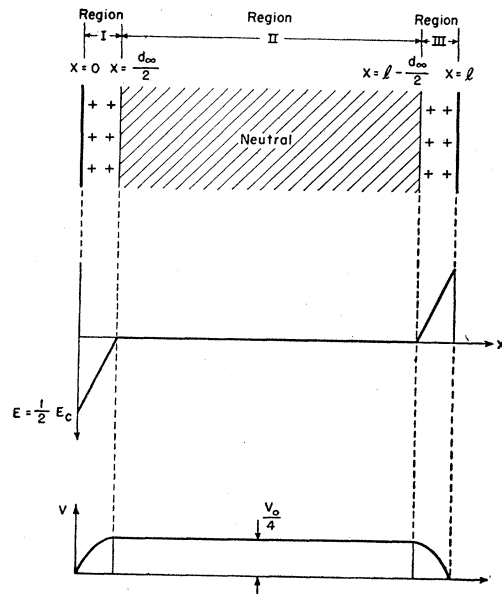


FIG. 4. Space-charge, field-strength, and voltage distribution after discharge (theoretical).

the unusual situation that the mobility b , and with it the time constant τ of the space-charge buildup, can be controlled from the outside by the color and intensity L_0 of the illumination.

The photoelectrons in the alkali halides, as Pohl and his co-workers^{4,5} found, travel, after release, an average distance \bar{w} towards the anode before they are retrapped. This drift distance increases proportionally to the driving-field strength, decreases with the concentration of color centers, and depends on the temperature, composition and prehistory of the sample. The drift distance per unit field strength, \bar{w}_0 , is short and of the order 10^{-11} [m/v]. If t_b and t_f designate the average time intervals during which an electron is bound or travels freely, the drift velocity may be written

$$\bar{v} = bE = [\bar{w}_0 / (t_b + t_f)]E. \quad (54)$$

Obviously, for our model, the time an electron stays bound is inversely proportional to the intensity of the releasing light,

$$t_b = 1/\beta L_0. \quad (55)$$

If this time is long compared with the time of free travel ($t_b \gg t_f$), as is normally the case, the mobility

$$b \simeq \bar{w}_0 / t_b \simeq \bar{w}_0 \beta L_0 \quad (56)$$

is proportional to the intensity of illumination.

The introduction of a mobility b into Eq. (54) presupposes that the internal field strength across the drift distance \bar{w} is constant. Since the drift distance \bar{w}_0 is very small and the field strength in region II does not exceed the applied field V_0/l , the assumption should be valid in this region. Difficulties may arise if the shock front is not the sharp boundary of our model, but diffuse because electrons have been left behind in the cathode fall. However, such stragglers, when liberated, find themselves in a much steeper field and tend to catch up with the main front speedily. Thus one may expect, just as in the Stasiw experiment on the thermal mobilization of electrons at high temperature,⁶ that the shock is sharply defined towards the cathode.

Real difficulties will arise for our simple model from other causes. Until now we have assumed the existence of only one type of trap, that characterized by the F -band absorption. Actually, we know that a variety of traps exist, starting with the F band of Pohl and co-workers⁷ and the M and R bands found by Molnar⁸ in this laboratory, to the broad, continuous absorptions of colloidal aggregates that form by irradiation with

with white light^{5,9} or during long-time storage of additively colored crystals. If the F centers are caused by Schottky defects and correspond, as de Boer suggested,¹⁰ to one electron attached to a negative ion vacancy, the F' centers, according to Pick's quantum efficiency measurements,⁷ may represent two electrons attached to such vacancy. The R and M centers, as Seitz proposed,¹¹ may correspond to two F centers side by side and to the combination of an F center with an anion-cation vacancy pair. Thus, while starting our experiment with a crystal containing only the F -band absorption, we are bound to produce, by illumination in this band, new trapping centers absorbing at longer wavelengths.^{9,11}

In consequence, if we mobilize the electron cloud by F -band illumination, we will leave electrons behind in other trapping centers as the shock front progresses. The effective space-charge density begins to fall below ρ_0 , and the relaxation time τ increases [see Eq. (25)]. Illumination at low temperature may delay the formation of these additional centers, as the yield characteristics of Pick indicate.⁷ This is understandable if the motion of Schottky defects and of vacancy pairs is a prerequisite for their formation.¹¹

White-light illumination will obviate some of these difficulties by remobilizing electrons trapped outside the F -band range. However, since the quantum yield from the R centers and from the colloidal centers is very low, we are found to lose electrons¹² as the experiment progresses.

5. FIELD EMISSION

When the field strength at the cathode builds up beyond some critical value, the probability rapidly increases that electrons enter by field emission. This effect will keep the gradient at the cathode lower than Eq. (7) prescribes, and a final current will flow; this requires that the field E_2 across the electron cloud does not drop to zero.

Field emission tends to take place at sensitive spots; and the distribution and efficiency of such spots is apt to alter as time goes on and to be affected in our case by the discharging of alkali metal.¹³ Neglecting this complication at present, we assume that the field-current density is prescribed by the field strength at the cathode as $J = J(E_c)$ and that it is carried through the crystal according to Stokes' law as

$$J(E_c) = \rho b E, \quad (57)$$

with the field gradient prescribed by Poisson's equation

$$\partial E / \partial x = (\rho + \rho_0) / \epsilon' \quad (58)$$

⁹ G. Glaser, Nachr. Ges. Wiss. Göttingen, Math.-physik. Kl. Fachgruppen II, 3, No. 2, 31 (1937).

¹⁰ J. H. de Boer, Rec. trav. chim. 56, 301 (1937).

¹¹ F. Seitz, Revs. Modern Phys. 18, 384 (1946).

¹² See in this connection the interesting observations of J. J. Oberly, Phys. Rev. 84, 1257 (1951); and of D. B. Dutton, Ph.D. thesis, University of Illinois, 1952 (unpublished).

¹³ A. von Hippel, Z. Physik 98, 580 (1936).

⁴ B. Gudden and R. Pohl, Z. Physik 31, 651 (1925); W. Flechsig, Z. Physik 33, 372 (1925); 46, 788 (1928); K. Hecht, Z. Physik 77, 235 (1932).

⁵ G. Glaser and W. Lehfeldt, Nachr. Ges. Wiss. Göttingen, Math.-physik. Kl. Fachgruppen II 2, 91 (1936).

⁶ O. Stasiw, Nachr. Ges. Wiss. Göttingen, Math.-physik. Kl. 261 (1932).

⁷ Cf. H. Pick, Ann. phys. 31, 365 (1938).

⁸ J. P. Molnar, Ph.D. thesis, MIT, 1940; Phys. Rev. 59, 944 (1941).

[see Eqs. (8) and (9)]. The initial current density at $t=0$ in the undistorted field is given [see Eq. (12)] as

$$J_0 = \rho_0 b V_0 / l; \quad (59)$$

hence the ratio of final current caused by field emission to initial current may be written

$$J(E_c) / J_0 = J(E_c) l / \rho_0 b V_0 \equiv -K. \quad (60)$$

We note that K is a negative number. By referring to the *relative* field strength, space-charge density, and distance,

$$E' = El / V_0, \quad \rho' = -\rho / \rho_0, \quad x' = x / l, \quad (61)$$

we may rewrite Eq. (58) for the discussion of the steady state

$$dE' / dx' = \alpha(1 - \rho'), \quad (62)$$

where [see Eq. (6)]

$$\alpha = l^2 \rho_0 / \epsilon' V_0 = 2l^2 / d_\alpha^2 \gg 1. \quad (63)$$

Since, according to Eqs. (57) and (60),

$$\rho' = K / E', \quad (64)$$

the Poisson equation becomes

$$\frac{dE'}{dx'} = \frac{d}{dx'} \left(-\frac{dV'}{dx'} \right) = \alpha \left(1 - \frac{K}{E'} \right), \quad (65)$$

with the boundary conditions:

$$\text{for } x' = 0, \quad E' = E_c / (V_0 / l); \quad (66)$$

$$\text{for } x' = 1, \quad V' = -\int_0^1 E' dx' = 1.$$

Integrating Eq. (65) we obtain

$$\frac{1}{2} E'^2 = -\alpha(V' + Kx') + A; \quad (67)$$

since the voltage $V' = 0$ at $x' = 0$,

$$A = \frac{1}{2} E_c'^2. \quad (68)$$

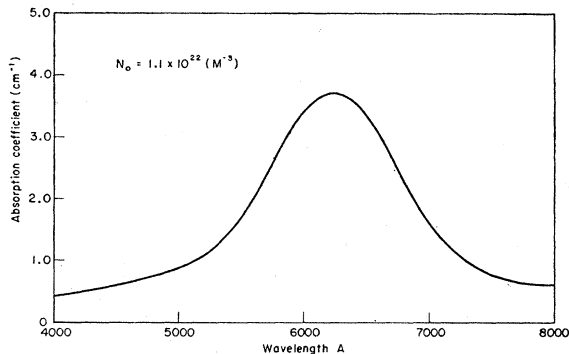


FIG. 5. Typical F -band absorption in colored crystal before experiment.

Rewriting Eq. (67) as

$$(1/\sqrt{2})(dV'/dx') = [A - \alpha(V' + Kx')]^{\frac{1}{2}}, \quad (69)$$

or

$$(2\alpha)^{\frac{1}{2}} dx' = \frac{dV'}{(A/\alpha - V' - Kx')^{\frac{1}{2}}}$$

and integrating once more we obtain the voltage distribution V' as $f(x')$ in the somewhat involved form,

$$-\frac{(2\alpha)^{\frac{1}{2}}}{2} x' = \left[\left(\frac{A}{\alpha} - V' - Kx' \right)^{\frac{1}{2}} - \left(\frac{A}{\alpha} \right)^{\frac{1}{2}} \right] - \frac{K}{(2\alpha)^{\frac{1}{2}}} \times \log \left[\frac{K/(2\alpha)^{\frac{1}{2}} + (A/\alpha - V' - Kx')^{\frac{1}{2}}}{K/(2\alpha)^{\frac{1}{2}} + (A/\alpha)^{\frac{1}{2}}} \right]. \quad (70)$$

By invoking the boundary condition [Eq. (66)], i.e., for $x' = 1$, $V' = 1$, we arrive at a relation between K , A and α as

$$-\frac{(2\alpha)^{\frac{1}{2}}}{2} = \left[\left(\frac{A}{\alpha} - 1 - K \right)^{\frac{1}{2}} - \left(\frac{A}{\alpha} \right)^{\frac{1}{2}} \right] - \frac{K}{(2\alpha)^{\frac{1}{2}}} \log \left[\frac{K/(2\alpha)^{\frac{1}{2}} + (A/\alpha - 1 - K)^{\frac{1}{2}}}{K/(2\alpha)^{\frac{1}{2}} + (A/\alpha)^{\frac{1}{2}}} \right]. \quad (71)$$

This expression can be reduced by approximation to an equation for the determination of the field gradient E_c at the cathode from a measurement of K , the ratio of final to initial current. In the case of no field emission, Eqs. (6), (7), and (63) specify that

$$(A/\alpha)^{\frac{1}{2}} = (E_c'^2 / 2\alpha)^{\frac{1}{2}} = 1, \quad (72)$$

or

$$E_c'(K=0) = (2\alpha)^{\frac{1}{2}}. \quad (73)$$

When field emission occurs, $(A/\alpha)^{\frac{1}{2}} < 1$ and $0 > K > -1$, and, since $\alpha \gg 1$, $|K|/(2\alpha)^{\frac{1}{2}} \ll 1$. The left side of Eq. (71) is large and negative; hence the argument of the logarithm on the right side must be positive and very close to zero, i.e.,

$$K/(2\alpha)^{\frac{1}{2}} + (A/\alpha - 1 - K)^{\frac{1}{2}} \ll 1,$$

or

$$A/\alpha - 1 - K \simeq K^2 / 2\alpha. \quad (74)$$

Since $K^2 / 2\alpha \ll 1$, Eq. (74) approximates to $2A \simeq (1+K)2\alpha$ or $E_c' \simeq (1+K)^{\frac{1}{2}}(2\alpha)^{\frac{1}{2}}$, that is,

$$E_c \simeq (1+K)^{\frac{1}{2}} E_c(K=0). \quad (75)$$

The field E_c of the cathode fall drops initially very slowly with K . For $K = -\frac{1}{2}$ it decreases to $0.71E_c(K=0)$. However, as K approaches -1 , i.e., when the final current approaches the initial current, the cathode fall begins to disappear, and for $K = -1$ the space-charge-free situation exists. Hence, by observing K and calculating $E_c(K=0)$ for no field emission, the gradient E_c at the cathode in the case of field emission may be obtained, and by plotting the final current $J(E_c)$ against E_c , the law of electron emission can be found.

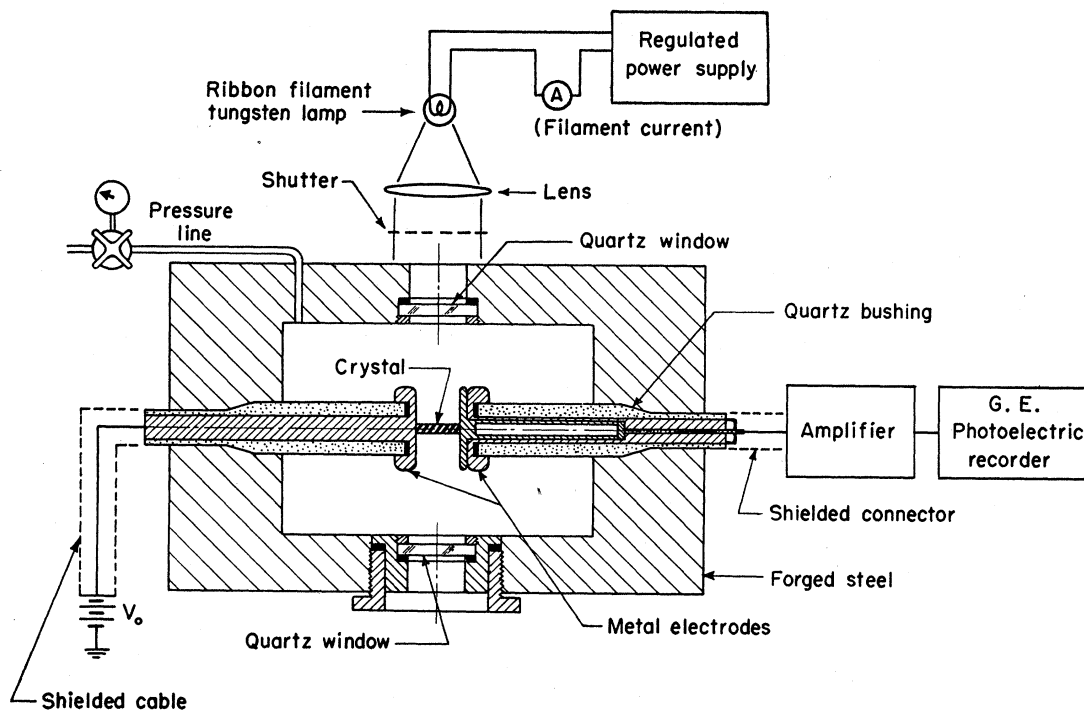


FIG. 6. Schematic view of equipment for photocurrent measurements.

6. EXPLORATORY EXPERIMENTS

To test the validity of our box model of the frozen-in electron gas, and to check on the field emission situation, a number of exploratory experiments were made at room temperature.

Samples and Equipment

As samples KBr crystals in the shape of rectangular bars were used, and colored either by the immigration of electrons at about 500°C or additively colored in alkali metal vapor. The vapor treatment was carried out in an iron tube placed in a two-stage furnace. The crystal was kept at high temperature (625°C) to reach equilibrium rapidly by diffusion, while the alkali metal in the low-temperature section determined, by its vapor pressure, the density of the color centers, N_0 [see Eq. (1)]. Rapid cooling by an air blast kept the electrons in their F -center traps, as a check of the optical absorption with a recording Cary spectrophotometer confirmed (Fig. 5). The density of F centers was calculated from the half-width of the F band according to Smakula's procedure;¹⁴ it was adjusted for our experiments from $ca\ 10^{20}$ to 10^{24} [m⁻³].

Gold electrodes were applied to the end surfaces of the samples by vacuum evaporation; and the crystals were inserted in a sample holder that allowed illumination from both sides and the application of gas pressure to suppress corona discharges (Fig. 6).

Three types of illumination were provided: (a) constant over-all illumination by a tungsten ribbon-filament

lamp; (b) a narrow light probe that could be focused on any part of the crystal and was modulated at 90 cps by a mechanical chopper; (c) a third light source that could project a slit of adjustable width on the crystal for any partial illumination desired.

The photocurrent as a function of time was measured with a feedback micromicroammeter (maximum sensitivity, $ca\ 10^{-13}$ amp full scale, noise level 10 percent of this value) connected to a G-E recorder. The ac system consisted of an electrometer tube amplifier, followed by a high-gain ac amplifier, tuned filter and output meter (maximum sensitivity about the same as that of the dc system). Batteries served as the voltage supply for the crystal current.

In the experiments reported here, the tungsten ribbon filament lamp (G-E 6 v, 18 amp) was used as the only light source. It has not yet been calibrated in absolute units as function of the lamp current; a relative intensity characteristic is included in Fig. 11. In the measurements reported in the subsequent section, the lamp current served as a measure of the light intensity.

Measurements and Results

A KBr crystal of medium color-center density ($N_0 \approx 10^{22}$ [m⁻³]), connected to a voltage of about 500 v and weakly illuminated by white light (8 amp), shows a current-time response, as indicated in curve (1) Fig. 7. Contrary to the expectations of our simple model (see Fig. 2), no straight line portion manifesting an exponential current decrease can be discerned, but only a rapidly arrested slope leading to a slightly

¹⁴ A. Smakula, Z. Physik 59, 603 (1930).

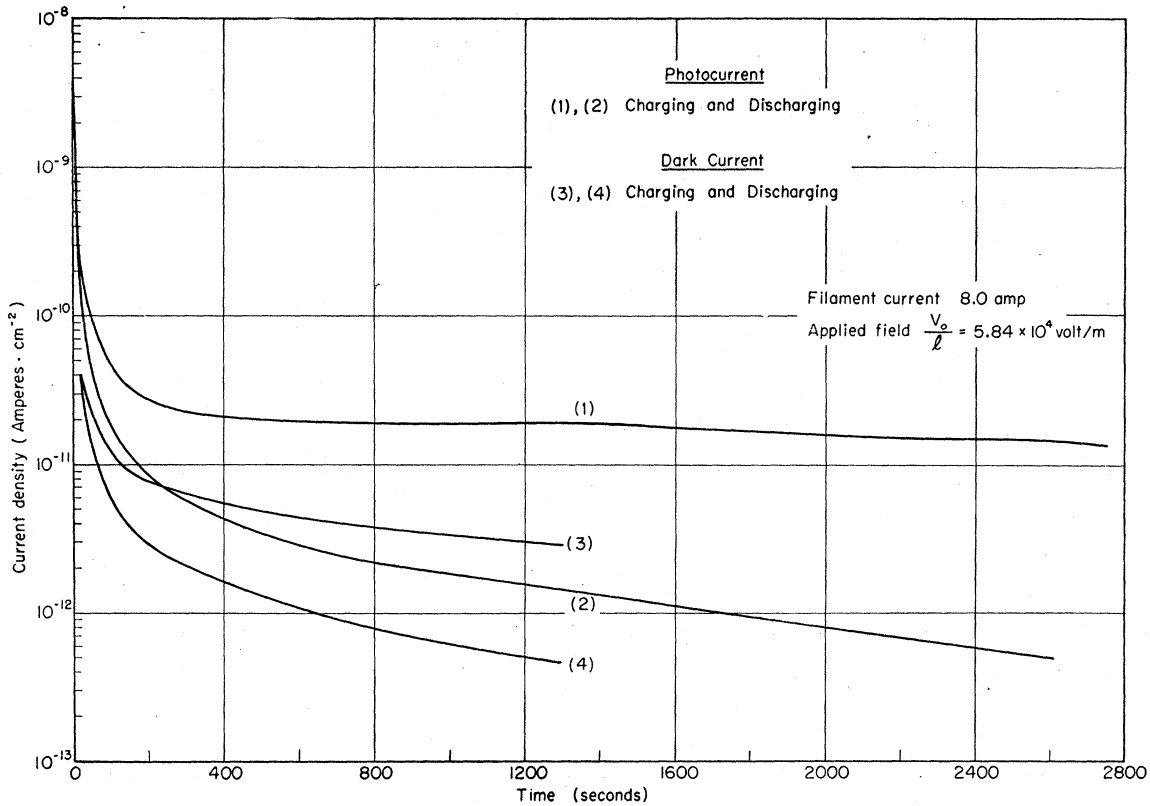


Fig. 7. Current density vs time for charging and discharging with and without illumination.

undulating final value. Repetition of the charging experiment produces similar curves with somewhat faster decay and lower final currents. The discharging characteristic (2) shows a still faster initial fall, followed by a long, sloping decrease over hours. Charging and discharging without illumination produces the same type of curves (3 and 4), displaced by about an order of magnitude to lower current values. The relatively large dark current in these first experiments is due to traces of moisture; in later measurements on freshly split crystals it is reduced by a factor of *ca* 100.

The situation is clarified when the charging and discharging curves are observed on a crystal of lower color-center density ($N_c \approx 5 \times 10^{21} \text{ [m}^{-3}\text{]}$) over a wide range of voltages (Fig. 8). For low voltage, the charging and discharging characteristics are really straight lines of nearly identical slope. For higher voltages the linear part of the charging curve systematically shortens and steepens, and the characteristic bends over rapidly to some constant current value. Simultaneously the discharging characteristic drops rapidly below that of the charging current.

The deviation from a straight line relation and the existence of a final current are factors indicating field emission. At a first glance, this explanation seems unlikely in view of the low voltages applied. However, according to our model [see Eqs. (6) and (7)], 22.5

volts across the crystal of Fig. 7 contract to a cathode fall of $d \approx 1.2 \times 10^{-6} \text{ [v} \cdot \text{m]}$ with a field gradient $E_c \approx 3.7 \times 10^7 \text{ [v} \cdot \text{m}^{-1}\text{]}$ in front of the electrode. We know from experience¹⁵ that such fields, not far below the breakdown strength, produce field emission. In charging, the emission sets in *after* the cathode fall has contracted sufficiently; a final state then is approached in which the emission from the cathode is balanced by the transconductance through the electron-cloud region II. In discharging, the electron cloud is pushed backwards, the gradient at the previous cathode is lowered rapidly, and the gradient at the previous anode is built up until field emission sets in also at that electrode. Zero current results when the gradient and field emission at both electrodes have become equal. The emission at the electrodes is expected to follow the law¹⁶

$$J = aE_c^2 e^{-b/E_c} \quad (76)$$

The indirect evidence for field emission just discussed can be confirmed by direct experimental proof. When field emission exists, electrons are drawn into the crystal even in the dark. They accumulate in front of the cathode, and are released in a current pulse when the light is suddenly switched on. Figure 9 gives an example

¹⁵ A. von Hippel, Phys. Rev. **54**, 1096 (1938).

¹⁶ R. H. Fowler and L. Nordheim, Proc. Roy. Soc. (London) **A119**, 173 (1928).

TABLE I. Time constant τ vs light intensity at 22.5 v.

Filament current (amp)	τ (sec)	J_0 (amp/cm ²)	$J_0\tau$ (coulomb/cm ²)
8	128	4.4×10^{-13}	5.6×10^{-11}
9	70	10^{-12}	7×10^{-11}
10	35	2.3×10^{-12}	8.1×10^{-11}
11	19	4.4×10^{-12}	8.3×10^{-11}
12	13	7.6×10^{-12}	9.9×10^{-11}
13	8	1.3×10^{-11}	10.4×10^{-11}
14	6	1.7×10^{-11}	10.2×10^{-11}

of such current pulses, measured as a function of dark-time interval and voltage. For the crystal shown, field emission can thus be clearly demonstrated at 4.5 v; for higher color-center densities we could establish field emission even below 1 v. When a crystal has been charged with sufficient voltage, such current pulses can be produced in discharge for many days and give, in their height, a good measure of the remaining field gradient.

Returning to the initial current density J_0 and the relaxation time τ of the space-charge buildup, we would expect that τ is inversely proportional to the light intensity [see Eqs. (26) and (56)], but that the product $J_0\tau$ is constant for a given crystal and charging

TABLE II. Variation of time constants with voltage, Crystal 12A, at 10 amp.

Volts	τ (sec)	I_0 (amp)
4.5	33.5	2×10^{-12}
22.5	21	1.1×10^{-11}
90	14	4.5×10^{-11}
300	9	1.5×10^{-10}

voltage. Table I confirms that this is the case within our limits of accuracy. Table II shows, in addition, that the initial current increases proportionally to the applied voltage, as predicted; the time-constant measurements for higher voltages are relatively inaccurate since the linear slopes are very short, hence the expected decrease of τ , as $(V_0)^{-\frac{1}{2}}$ can only be surmised. Similarly Table III, for the same reason, cannot confirm accurately that τ varies proportionally to $(N_0)^{-\frac{1}{2}}$, but shows the expected trend. The pen recorder is being replaced presently by a cathode-ray oscillograph for more accurate slope measurements.

Seen from the standpoint of photoelectric response, our crystals represent a *new type of photocell*. Ordinarily,

TABLE III. Variation of time constant with color density at 22.5 v and 10 amp.

Crystal	N_0/cm^3	τ (sec)
13B	2×10^{14}	35
12A	8.6×10^{14}	21
10A	4.3×10^{15}	7

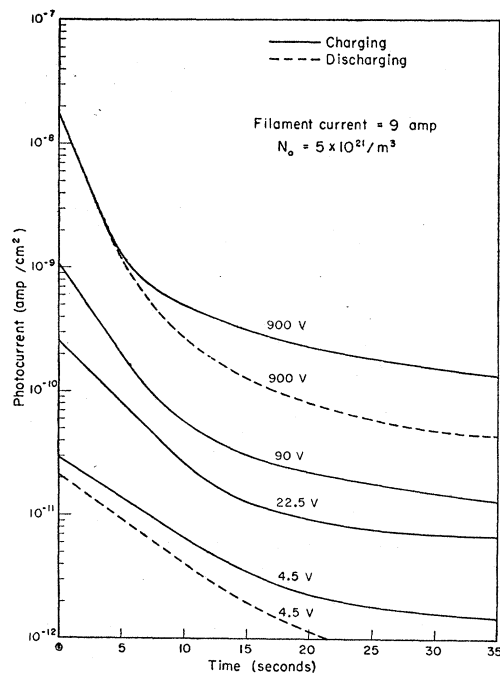


FIG. 8. Photocurrent curves at different voltages for constant light intensity.

the photoeffect in solids is either composed of the electrons directly liberated by the absorbed quanta (*primary photoeffect*) or results from a change in the conductivity of the dielectric induced by the light absorption (*secondary photoeffect*). A distinction between these two effects, based on the speed and yield of the response, was made by Gudden and Pohl¹⁷ at an early date. The primary photoeffect, represented, for example, by the *F*-center electrons mobilized by light absorption, responds instantaneously and can usually

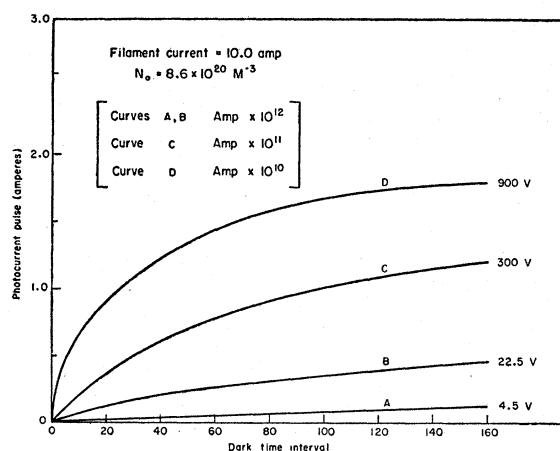


FIG. 9. Photocurrent pulse as function of dark-time interval and voltage.

¹⁷ See B. Gudden, *Lichtelektrische Erscheinungen* (Verlag. Julius Springer, Berlin, 1928).

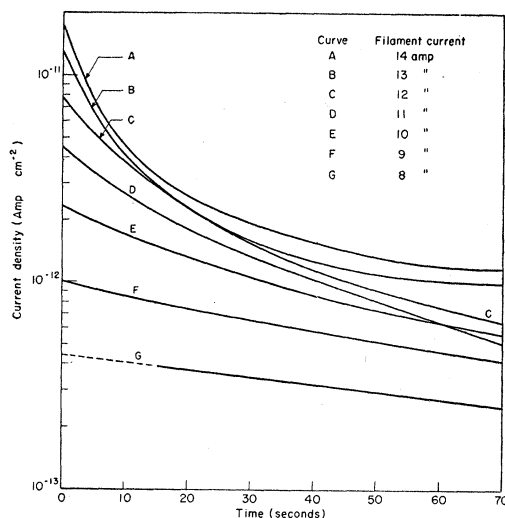


FIG. 10. Charging characteristics for different light intensities ($V_0 = 22.5$ v, $N_0 = 2 \times 10^{20}/\text{m}^3$).

not exceed one electron per absorbed quantum. The secondary photocurrent, exemplified, for instance, by the thallose sulfide photocell,¹⁸ responds sluggishly, but can reach much larger quantum yields.

In our experiments of controlled space-charge build-up, first a normal primary photoeffect occurs. When the stationary state is reached without field emission, the bleached cathode fall (region I of Fig. 1) is free of F centers, and the colored region II of the electron cloud, free of field. Hence, while photoelectrons are still being liberated in region II, they acquire no drift velocity towards the anode, and the current ceases.

The situation changes when electrons are taken in at the cathode. This may be accomplished by the normal external photoeffect, well known from gas and vacuum photocells. The energy required to transfer an electron from silver into KBr photoelectrically has been investigated recently by Gillo¹⁹ in this laboratory and amounts to about 4.3 eV. This external photoeffect actually occurs in our experiments under strong white-light illumination, as Fig. 10 indicates. If a crystal of very low color-center density is illuminated by the tungsten lamp raised only to yellow heat (curve G, 8 amp), a straight, exponential, current decay is observed at low voltage indicating no emission. As the temperature of the light source is increased, the characteristics bend over systematically to higher and higher constant values. Simultaneously, the initial slopes steepen as predicted by our model, because the mobility b of the F electrons in the crystal increases proportionally to the light intensity [see Eq. (56)], hence the time constant shortens. These curves are similar to those obtained by field emission, but that they originate from external photoeffect can be established beyond

¹⁸ A. von Hippel and E. S. Rittner, *J. Chem. Phys.* **14**, 370 (1946).

¹⁹ M. A. Gillo, this issue [*Phys. Rev.* **91**, 534 (1953)].

doubt. The photoresponse is greatly reduced when the blue part of the light beyond the F -band region is cut out by filters;²⁰ furthermore, no electrons accumulate in dark-time intervals which could be released as current pulses.

In the region of field emission, this external photocurrent is overshadowed by the field current; the strong photosensitivity now appearing (Fig. 11) is due to the delicate balance between the field strength at the cathode, regulating the emission, and the voltage gradient in the electron cloud (region II), providing for the electron transport to the anode. With increasing light intensity, the mobility of the electrons in this region rises; the voltage gradient required for the current transport diminishes, and field can be retracted to the cathode, until the increasing emission establishes a new balance at a higher current value.

This new photocell type, that responds to illumination changes by changes in field distribution and thus in

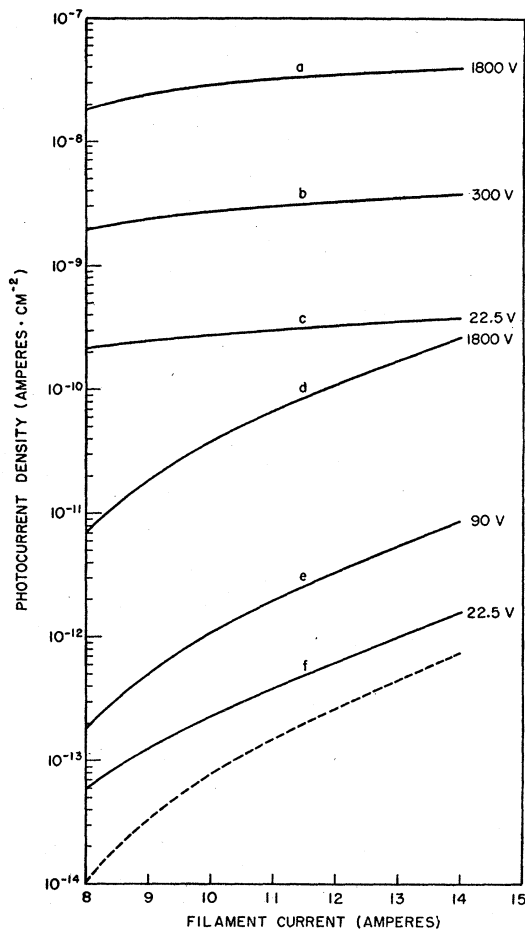


FIG. 11. Photocurrent as function of light intensity. Curves a, b, c : $N_0 = 1.1 \times 10^{23} \text{ m}^{-3}$; curves d, e, f : $N_0 = 2 \times 10^{20} \text{ m}^{-3}$; --- intensity of light source in F -band region (arbitrary units).

²⁰ In our crystals some potassium is deposited at the cathode by ionic migration as the experiment continues, hence some sensitivity to larger wavelengths remains.

field emission, may properly be called a "field-emission photocell." It has some peculiar properties. Since the relaxation time τ is inversely proportional to the mobility [see Eq. (25)], the cell becomes sensitive to higher frequencies as the light intensity increases. Furthermore, since the voltage gradient required for the transport of current is inversely proportional to the color-center density, a lighter colored crystal is more sensitive to illumination changes, because more voltage can be reflected towards the cathode. Finally, we have observed that the photosensitivity can be extended by building in new absorption centers in other spectral regions, for example, in the infrared.

In Eq. (75) we show how the true field gradient E_e at the cathode may be found from the ratio of initial-to-final current. The law of electron emission can thus be established. No quantitative comparison has been made at the present time because the emission experimentally observed is not uniformly distributed over

the cathode surface but takes place from sensitive spots. If we could observe it visually, it would resemble a scintillation phenomenon, with spots becoming active and inactive, changing shape and emissivity as time goes on. The field emission current is therefore noisy, but the noise diminishes as the cathode becomes conditioned. We believe that this is the noise observed in pre-breakdown currents by Haworth and Bozorth,²¹ by us,¹⁵ and recently again by Kawamura and Omuki,²² and that it should probably not be interpreted as the sign of pre-breakdown avalanches.

The authors are greatly indebted to D. A. Powers for the design of the micromicroammeter, to L. B. Smith for the design of the high-pressure sample holder, and to J. Kalnajs for the preparation of the colored crystals.

²¹ R. M. Bozorth and F. E. Haworth, Phys. Rev. **39**, 845 (1932).

²² H. Kawamura and M. Omuki, J. Phys. Soc. Japan **6**, 283 (1951).

Current Carrier Mobility Ratio in Semiconductors

L. P. HUNTER

International Business Machines Corporation, Poughkeepsie, New York

(Received April 3, 1953)

The ratio of the electronic mobility to the hole mobility in germanium has been reported by many workers. The ratio reported is usually obtained by measurements on two different samples of different conductivity types. The method suggested here deduces the mobility ratio from resistivity measurements made on a single sample. An accurate plot of resistivity as a function of temperature is made. The extrinsic and intrinsic branches of this curve are extrapolated to their intersection. If r is defined as the ratio of the resistivity of this intersection point to the measured resistivity at the same temperature, the quantity $[1/(r-1)-r]$ gives the mobility ratio for P type samples, and its reciprocal for N type samples.

IN the past few years a great many measurements of current carrier mobility in semiconductors have been reported.¹⁻⁵ The values reported show considerable disagreement, especially between values deduced from Hall effect measurements and those obtained from measurement of the drift velocity of injected carriers. This discrepancy has been noted and several mechanisms¹ suggested to account for it.

The ratio of the mobility of electrons to the mobility of holes in germanium may be computed from these various mobility values reported, and the best data presently available seems to give a value of about 2.1 for drift measurements¹ and a value of about 1.5 for Hall effect measurements.³ In all of these measurements the mobility values for electrons and holes were ob-

tained on different samples, of different conductivity types, at different times. Because of their nature, no direct measurements of the mobility ratio were made on a single sample under a single set of conditions.⁶

The purpose of this paper is to suggest a method of measuring the mobility ratio directly using a single sample of either conductivity type. In Fig. 1 is shown a typical curve of the logarithm of resistivity *versus* the reciprocal of the absolute temperature. The two branches of this curve are extrapolated to their intersection point. This intersection point determines a resistivity value, ρ_e , and a temperature, T_0 . At the temperature T_0 the resistivity value of the measured curve ρ_0 is determined. If the ratio, $r = \rho_e/\rho_0$, is formed, it will be shown that for P type samples the mobility

¹ J. R. Haynes and W. Shockley, Phys. Rev. **81**, 835 (1951).

² Lark Horowitz, Middleton, Miller, and Walerstein, Phys. Rev. **69**, 258 (1946).

³ W. C. Dunlap, Phys. Rev. **79**, 286 (1950).

⁴ Esther M. Conwell, Proc. Inst. Radio Engrs. **40**, 1327 (1952).

⁵ G. L. Pearson and J. Bardeen, Phys. Rev. **75**, 865 (1949).

⁶ W. Shockley, *Electrons and Holes in Semiconductors* (D. Van Nostrand Company, Inc., New York, 1950), p. 218, problem 7 suggests a method of determining the mobility ratio for P type samples under the assumptions of equal Hall and drift mobility ratios and zero carrier lifetime. These assumptions are, in general, invalid [see R. Landauer and J. Swanson this issue, Phys. Rev. **555** (1953)].